International Journal for Multidisciplinary Research (IJFMR)
E-ISSN: 2582-2160 ● Website: www.ijfmr.com ● Email: editor@ijfmr.com

Analysis on Fabrication of AlN/GaN/AlN Quantum-Well THz Devices with a Phononic–Excitonic–Radiative Model

Htar Ei Hlaing[1], Lei Lei Yin Win[2], Thanda Win[3], Hla Myo Tun[4]

[1,2,3,4]Department of Electronic Engineering, Yangon Technological University, Myanmar

Abstract:
AlN/GaN/AlN quantum wells offer a compelling materials platform for terahertz (THz) device fabrication, combining an ultra-large conduction-band offset, LO-phonon energies sufficient to suppress thermal backfilling, and excitonic resonances that can be engineered through confinement. This paper presents a fabrication-oriented model that integrates phononic, excitonic, and radiative design considerations into a coherent process flow. We first establish the physical rationale for the AlN/GaN/AlN double-barrier architecture, emphasizing the role of the 92 meV GaN LO phonon in enabling high-temperature THz operation and the influence of phonon screening on excitonic states in atomically thin wells. A fabrication sequence is then detailed, covering plasma-assisted molecular beam epitaxy with indium-surfactant-assisted interface engineering, ex situ characterization by high-resolution X-ray diffraction and transmission electron microscopy, and device processing into mesa-isolated resonant-tunneling and intersubband structures. We propose a phononic–excitonic–radiative co-design methodology in which LO-phonon scattering rates, exciton binding energies, and intersubband oscillator strengths are evaluated self-consistently before growth, and we discuss how measured structural parameters feed back into the model. Critical challenges—including interface roughness, polarization-induced field nonuniformity, and the trade-off between barrier thickness and tunneling current—are analyzed. The model provides a practical route toward reproducible AlN/GaN/AlN THz devices and identifies the metrology and modeling gaps that must be closed for room-temperature operation.

Keywords: AlN/GaN/AlN, quantum well, terahertz, molecular beam epitaxy, phonon, exciton, intersubband

1. Introduction

The terahertz spectral window, conventionally spanning 0.1–10 THz, remains one of the least developed regions of the electromagnetic spectrum despite decades of recognized potential in imaging, spectroscopy, and secure communications. The central obstacle is the absence of compact, room-temperature solid-state sources and detectors with adequate performance. GaAs-based quantum cascade lasers have demonstrated THz emission, but their operation is confined to cryogenic temperatures because the longitudinal-optical (LO) phonon energy of GaAs (36 meV) is too small to prevent thermal population of the lower laser state at elevated temperatures [1-2].

III-nitride semiconductors have long been identified as a materials system that could circumvent this limitation. GaN possesses an LO-phonon energy of approximately 92 meV, roughly 2.5 times that of

GaAs, which suppresses phonon-mediated thermal backfilling and opens a path toward THz devices operating at or near room temperature. Equally important, the GaN/AlN heterojunction provides a conduction-band offset of approximately 1.4–1.8 eV, the largest among common semiconductor heterostructures, enabling deep quantum confinement and wide tunability of intersubband transition energies [3-4].

The AlN/GaN/AlN double-barrier quantum well, in particular, has emerged as a structurally simple yet physically rich platform. Resonant tunneling diodes based on this architecture have exhibited room-temperature negative differential resistance with peak current densities exceeding 10^3 kA/cm² and peak-to-valley current ratios above 1.2. Intersubband absorption in AlN/GaN multiple quantum wells has been tuned from the near-infrared to wavelengths as long as 63 μm, corresponding to frequencies below 5 THz. These results establish the basic feasibility of AlN/GaN/AlN quantum wells as THz-active elements [5-6].

What has been less developed is a fabrication methodology that explicitly accounts for the coupled phononic, excitonic, and radiative physics of these structures. In nitride quantum wells, the same LO phonons that enable high-temperature operation also govern non-radiative relaxation rates that determine population inversion feasibility. Excitonic effects, enhanced by the large effective masses and strong confinement in nitrides, modify the optical response in ways that are only beginning to be understood; recent ab initio work has shown that phonon screening from AlN barriers can substantially alter the lowest exciton in monolayer GaN wells. Radiative processes—both intersubband emission and spontaneous recombination—depend sensitively on the precise layer thicknesses and interface quality achievable by epitaxy [7-10].

This paper addresses that gap by presenting a fabrication model organized around the phononic–excitonic–radiative model. Rather than treating growth, processing, and device physics as separate domains, we propose an integrated approach in which the three physical channels are evaluated before, during, and after fabrication, with measured structural parameters serving as inputs to refined physical models. Section 2 develops the physical basis of the model. Section 3 details the fabrication process, from substrate preparation through device isolation. Section 4 presents the characterization strategy that links structural metrology to model validation. Section 5 discusses the principal fabrication challenges and the trade-offs they impose. Section 6 concludes with an assessment of the most promising directions for future work.

2. Phononic–Excitonic–Radiative Model

2.1 Phononic Subsystem

The phononic behavior of AlN/GaN/AlN quantum wells is dominated by the LO phonon of GaN at approximately 92 meV. In the context of THz device design, this energy serves two opposing functions. On one hand, it provides a large “phonon bottleneck”: the energy separation between the upper and lower laser states in a quantum cascade design can be set below the LO-phonon energy, preventing rapid non-radiative depopulation of the upper state and preserving population inversion to higher temperatures than is possible in GaAs-based devices. On the other hand, resonant LO-phonon scattering is precisely the mechanism exploited for rapid depopulation of the lower state, and its rate must be engineered to be fast

enough to maintain inversion while not so fast that it degrades the upper-state lifetime through parasitic channels.

In the AlN/GaN/AlN double-barrier structure, interface phonons introduce additional complexity. The AlN barriers support their own phonon modes at higher energies (the AlN LO phonon is approximately 110 meV), and the overlap of confined and interface phonon modes with the electron wavefunction in the GaN well determines the actual scattering rates. These rates are not simply bulk-like; they depend on the well width, the barrier thickness, and the interface abruptness. For the thin wells (2–5 nm) typical of THz designs, the electron–phonon interaction enters the strong-coupling regime, and the simple Fröhlich Hamiltonian must be augmented by confined and interface mode contributions.

Recent theoretical work has highlighted an additional phononic effect relevant to the excitonic channel: phonon screening of the electron–hole interaction. In atomically thin GaN wells embedded in AlN, specific phonons in the AlN barriers can screen the Coulomb attraction between confined electrons and holes, substantially modifying exciton binding energies and optical transition energies. This effect is absent from standard effective-mass models and must be incorporated into any predictive model of the well's optical response.

2.2 Excitonic Subsystem

Excitons in nitride quantum wells are robust entities. The large electron and hole effective masses in GaN (approximately 0.20 m_0 and 1.0 m_0, respectively) and the strong quantum confinement in thin wells produce binding energies that can exceed 50 meV, well above room-temperature thermal energy. In the AlN/GaN/AlN system, the situation is complicated by the polarization-induced electric field.

For c-plane growth, spontaneous and piezoelectric polarization discontinuities at the AlN/GaN interfaces generate internal fields of several MV/cm. These fields spatially separate electrons and holes within the well, reducing the exciton binding energy and producing a pronounced quantum-confined Stark effect. The exciton transition energy therefore depends sensitively on well width and barrier composition, and this dependence must be accounted for in any design that seeks to exploit excitonic resonances for THz generation or detection.

The excitonic channel contributes to THz device physics in two ways. First, excitonic resonances can enhance the optical nonlinearity near the band edge, which is relevant for optically pumped THz emission schemes. Second, the exciton population dynamics—formation, dissociation, and recombination—couple to the phonon bath and to the free-carrier population that participates in intersubband transitions. A fabrication process that introduces unintended interface roughness or compositional grading will broaden excitonic features and degrade this coupling.

2.3 Radiative Subsystem

The radiative channel encompasses both intersubband emission (the desired output for a THz source) and interband spontaneous emission (a loss channel in most THz designs). For intersubband devices, the relevant quantity is the oscillator strength of the transition between confined electron subbands, which depends on the overlap integral of the initial and final state wavefunctions. This overlap is maximal when

the well is symmetric and the interfaces are abrupt; any asymmetry from polarization fields or interface roughness reduces the oscillator strength.

The radiative rate for intersubband transitions is intrinsically small compared to non-radiative rates, which is why THz quantum cascade lasers require careful waveguide design to achieve sufficient modal gain. In the AlN/GaN/AlN system, the large LO-phonon energy means that non-radiative lifetimes can be long at low temperatures but shorten rapidly as the temperature rises and LO-phonon emission becomes thermally activated. The temperature dependence of the radiative efficiency is therefore governed by the phononic subsystem, completing the coupling that gives the model its name.

2.4 Coupling of Subsystems

The three subsystems are not independent. The phononic channel determines non-radiative lifetimes that compete with radiative emission. The excitonic channel modifies the effective band structure and the available density of states. The radiative channel depends on the wavefunction overlap that is itself influenced by the polarization fields and interface quality established during fabrication.

A practical implementation of the model for fabrication purposes proceeds as follows. Before growth, the target device specification (e.g., emission at 3 THz, or resonant tunneling peak at 0.8 V) is translated into required subband energies using a self-consistent Schrödinger–Poisson solver that includes polarization charges. The phononic scattering rates between relevant subbands are then computed using a dielectric continuum model that accounts for confined and interface modes. The excitonic correction to the optical transition energies is estimated from a variational calculation with phonon screening included as a perturbation. Finally, the expected radiative efficiency is computed from the ratio of the radiative rate to the total (radiative plus phononic) rate. The output of this pre-growth modeling is a set of target layer thicknesses and compositions, together with a tolerance budget for interface roughness and compositional grading.

3. Fabrication Process

3.1 Substrate Selection and Preparation

The choice of substrate exerts a first-order influence on the quality of AlN/GaN/AlN quantum wells. Freestanding GaN substrates offer the lowest dislocation densities (below 10^6 cm^{-2}) and the best thermal matching to the active region, but their cost and limited availability constrain their use to applications where performance justifies the expense. GaN-on-sapphire templates grown by metal-organic chemical vapor deposition (MOCVD) provide a cost-effective alternative and have been used successfully for AlN/GaN resonant tunneling diodes with excellent DC characteristics. For THz devices where waveguide loss and heat dissipation are critical, the thermal conductivity of the substrate matters; sapphire's relatively low thermal conductivity (approximately 35 W/m·K at room temperature) compared to GaN (approximately 130 W/m·K) can lead to self-heating in high-current-density devices.

The substrate preparation sequence for plasma-assisted molecular beam epitaxy (PA-MBE) begins with degreasing in organic solvents, followed by an acid etch to remove native oxide, and immediate loading into the growth chamber. In situ thermal cleaning under nitrogen plasma at 700–800°C removes residual

carbon and oxygen, as confirmed by reflection high-energy electron diffraction (RHEED) showing a sharp (1×1) pattern.

3.2 Epitaxial Growth by PA-MBE

The active region—a GaN quantum well sandwiched between AlN barriers—is grown by PA-MBE. The choice of MBE over MOCVD is motivated by the need for atomic-level control of interface abruptness, which is difficult to achieve in MOCVD due to gas-phase memory effects and the higher growth temperatures that promote interdiffusion. MBE growth of AlN/GaN superlattices has been demonstrated with interface widths below 1 nm, as verified by transmission electron microscopy.

A critical innovation in recent AlN/GaN/AlN growth is the use of indium as a surfactant. Zhang et al. demonstrated that introducing a small indium flux during the growth of the AlN/GaN/AlN double-barrier structure reduces interface roughness and suppresses elemental interdiffusion, resulting in resonant tunneling diodes with record peak current density and improved reproducibility. The indium is believed to segregate to the growth front, enhancing adatom mobility and promoting layer-by-layer growth without incorporating significantly into the nitride film. This technique is incorporated into the baseline process flow described here.

The growth sequence for a single quantum well is as follows. After a GaN buffer layer (typically 500 nm–1 μm) grown at 800°C, the substrate temperature is reduced to approximately 720°C for the AlN barrier. The lower AlN barrier (thickness 1.5–3 nm) is grown at a rate of approximately 0.1 ML/s with a V/III ratio sufficient to maintain stoichiometry. The GaN well (thickness 2–5 nm) is then grown, followed by the upper AlN barrier. The indium surfactant flux is maintained throughout the barrier and well growth. RHEED intensity oscillations are monitored to confirm layer-by-layer growth and to calibrate thicknesses in situ.

For multiple-quantum-well structures intended for intersubband absorption or emission, the period is repeated 20–100 times, with a GaN spacer layer separating adjacent wells to prevent electronic coupling. The spacer thickness must be chosen to be thick enough to decouple the wells but thin enough to maintain strain balance; typical values are 5–10 nm.

3.3 Structural Characterization

Ex situ characterization begins with high-resolution X-ray diffraction (HRXRD). Symmetric (0002) rocking curves provide information on the periodicity and average composition of the superlattice, while asymmetric reciprocal-space maps reveal the strain state of the AlN barriers and GaN wells. For a well-designed structure, the superlattice satellite peaks should be sharp and numerous, indicating reproducible periodicity.

Cross-sectional transmission electron microscopy (TEM) provides direct imaging of the interface quality. High-angle annular dark-field (HAADF) imaging is particularly useful for distinguishing AlN from GaN due to the Z-contrast between Al and Ga. The TEM analysis should confirm that the well and barrier thicknesses match the design values within ±0.2 nm and that the interfaces are free of extended defects.

Atomic force microscopy (AFM) of the as-grown surface yields the root-mean-square roughness, typically 0.2–0.5 nm for optimized growth. Surface pits or step bunches visible in AFM are correlated with threading dislocations and must be minimized to reduce non-radiative recombination and interface scattering.

3.4 Device Processing

For resonant tunneling diode structures, the processing sequence begins with mesa isolation by chlorine-based inductively coupled plasma etching. The etch depth must penetrate through the active region into the underlying n^+-GaN contact layer. Ohmic contacts to the top and bottom n^+-GaN layers are formed by Ti/Al/Ni/Au metallization followed by rapid thermal annealing at 800–850°C in a nitrogen ambient. The contact resistance is measured by transmission line method (TLM) structures fabricated alongside the devices; values below 1×10^{-6} Ω·cm² are required for high-current-density operation.

For intersubband devices requiring optical access, a different processing route is used. A metal-insulator-metal waveguide can be formed by depositing a bottom metal layer (Ti/Au), defining the active mesa by dry etching, and then depositing a top metal layer. The insulator (typically Si_3N_4 or SiO_2) is deposited by plasma-enhanced chemical vapor deposition and patterned to open a window for optical coupling or electrical injection. For surface-plasmon waveguides, the top metal is patterned into a grating to facilitate outcoupling of THz radiation.

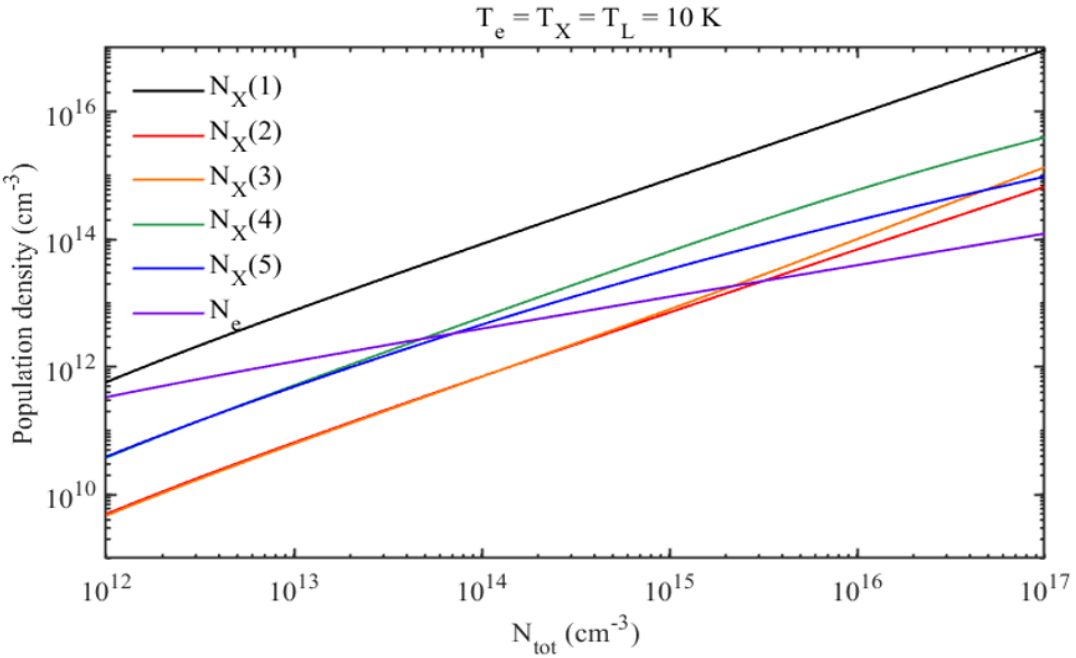
In all cases, the processing temperature after active region growth must be kept below the point at which interdiffusion becomes significant. Studies of AlN/GaN multiple quantum wells grown by MOVPE have shown that lowering the growth temperature suppresses interdiffusion and produces a blueshift of the intersubband absorption wavelength, confirming the sensitivity of the interface to thermal budget. For MBE-grown structures, the thermal budget of post-growth processing is generally less constrained, but annealing steps above 900°C should still be minimized.

4. Characterization and Model Validation

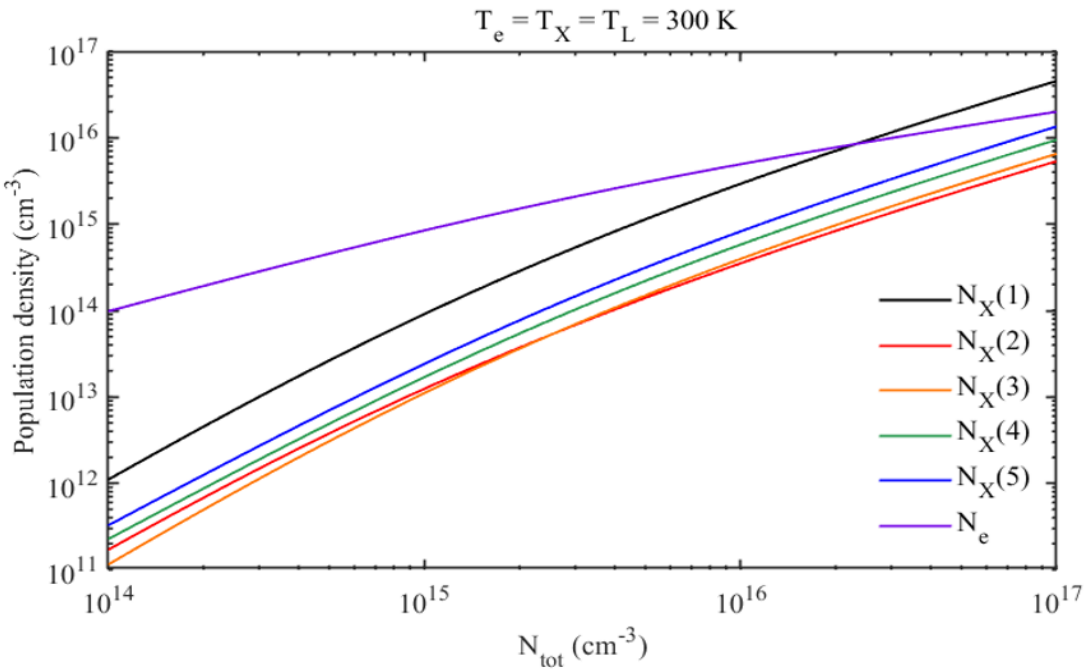
The phononic–excitonic–radiative model is only useful for fabrication if its predictions can be tested against measurable quantities. We propose a three-tier characterization strategy that maps onto the three subsystems.

For the Phononic characterization, Raman spectroscopy provides direct access to the phonon spectrum. The GaN E_2(high) mode at approximately 570 cm^{-1} and the A_1(LO) mode at approximately 735 cm^{-1} are the primary signatures. In a superlattice, the confined and interface phonon modes appear as additional features whose frequencies depend on the layer thicknesses. Comparison of the measured Raman spectrum with calculated phonon dispersion relations validates the structural parameters used in the scattering-rate model.

The horizontal axis is total density, and the vertical axis is the population of each state. The figures show how excitons are distributed among different energy states as the total density increases. The population behavior changes with temperature because the occupation of bound states and the continuum is temperature-dependent.



(a) QW at 10 K



(b) QW at 300 K

Figure.1. Calculated Population Distributions in the Quantum Well at Two Temperatures

At 10 K, the 1S population grows strongly in both materials as total density increases. The excited bound states remain below 1S at high density. At 300 K, more population stays in the excited states and the continuum.

The main difference is seen at 300 K: in the QW, the 1S and continuum populations become equal at about 2.3267×10^{16} cm^{-3}.

For the Excitonic characterization, Photoluminescence (PL) spectroscopy at temperatures from 10 K to room temperature reveals the excitonic transition energy and its temperature dependence. The PL linewidth is a sensitive probe of interface roughness and compositional inhomogeneity. Time-resolved PL provides the exciton lifetime, which is determined by the competition between radiative recombination and non-radiative channels (including phonon-assisted processes). The measured lifetime can be compared directly with the model's prediction.

Figure.2 (a) shows phonon-assisted deexcitation from 2S–5S to 1S; Figure.2(b) shows phonon-assisted formation of 1S excitons from the continuum. Both are plotted against phonon temperature, T_p.

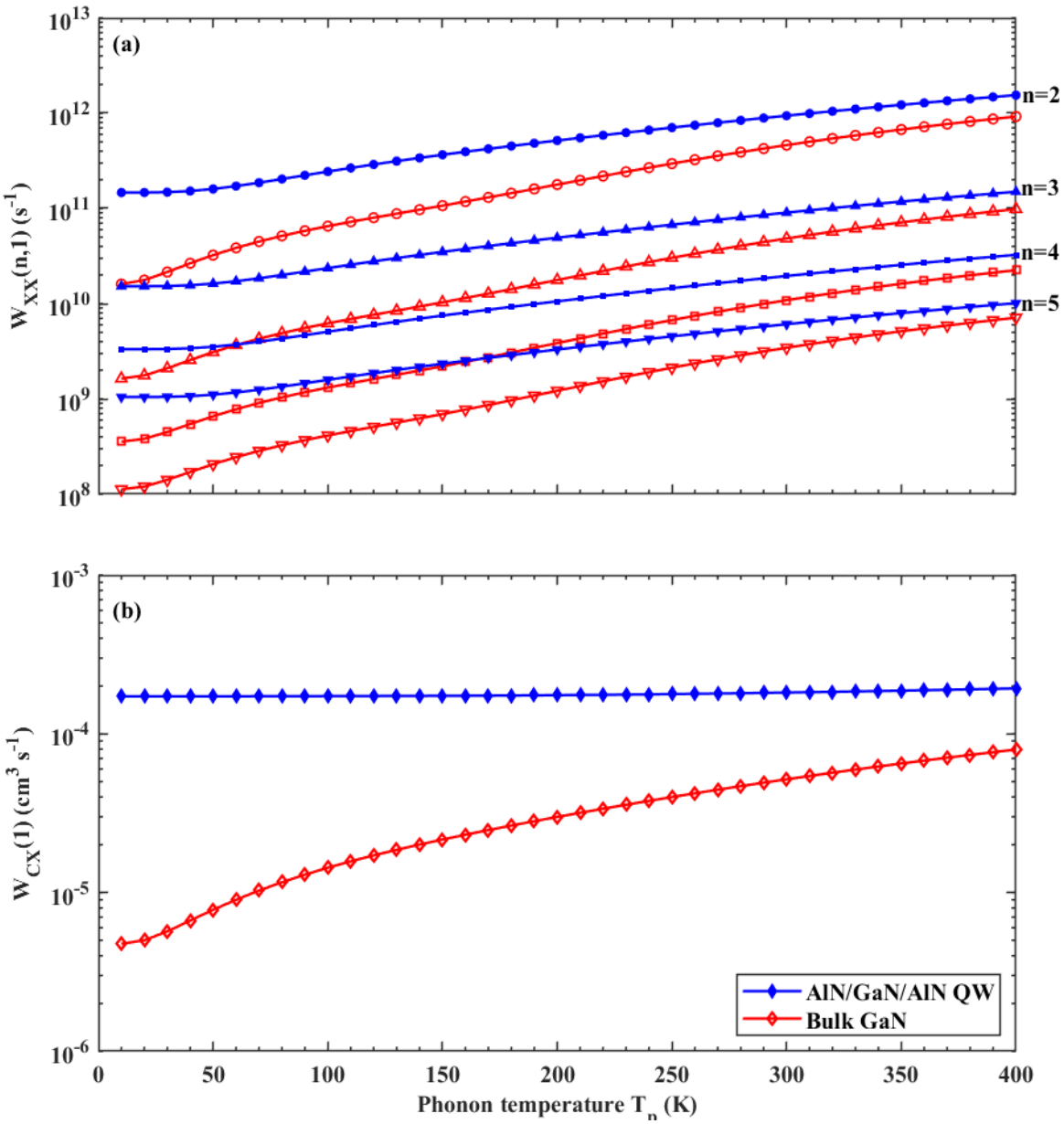


Figure.2 (a). Phononic Deexcitation Coefficients; (b) Continuum-to-1S Phononic Formation Coefficient

For the Radiative characterization with intersubband devices, Fourier-transform infrared (FTIR) transmission spectroscopy in a multipass waveguide geometry measures the intersubband absorption

spectrum. The peak position, linewidth, and oscillator strength are extracted and compared with the Schrödinger–Poisson calculation. For resonant tunneling diodes, current–voltage measurements at temperatures from 77 K to 300 K yield the peak voltage, peak current density, and peak-to-valley ratio. The temperature dependence of the peak current provides information on the dominant scattering mechanism, which can be compared with the phononic model's prediction.

Figure.3 (a) gives the electron-collisional deexcitation coefficients C(n,1) for transfers from higher bound states to 1S. Figure.3 (b) shows the continuum-to-bound-state formation coefficients α(n) for n = 1–5.

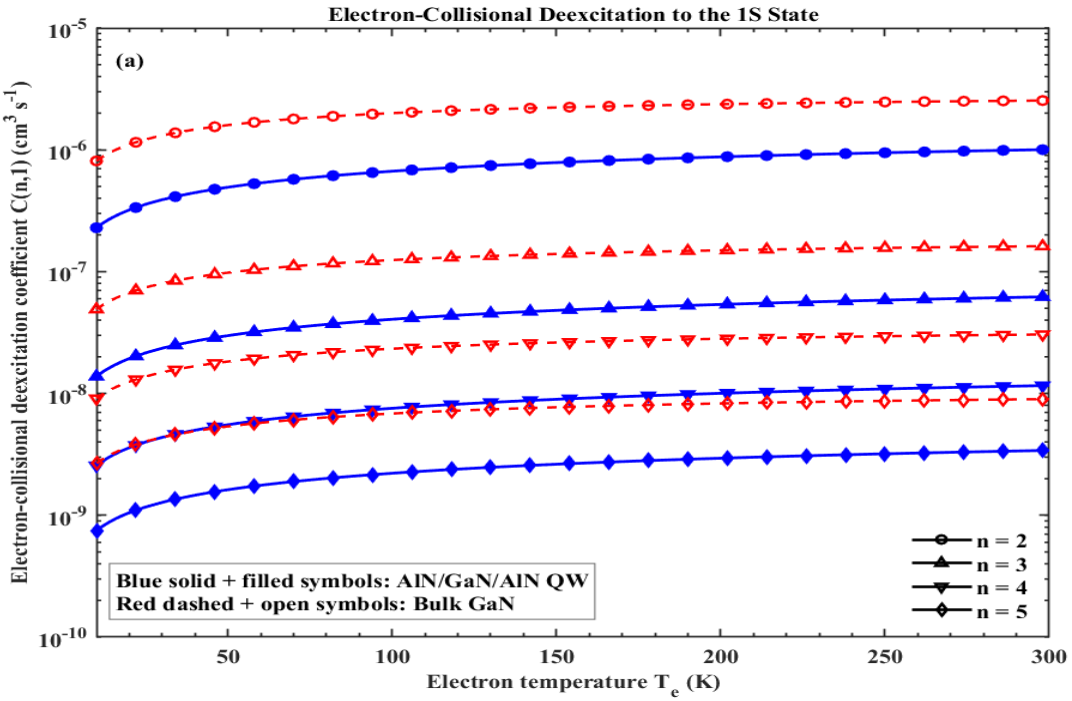


Figure.3 (a). Electron-Collisional Deexcitation Coefficients Versus Electron Temperature

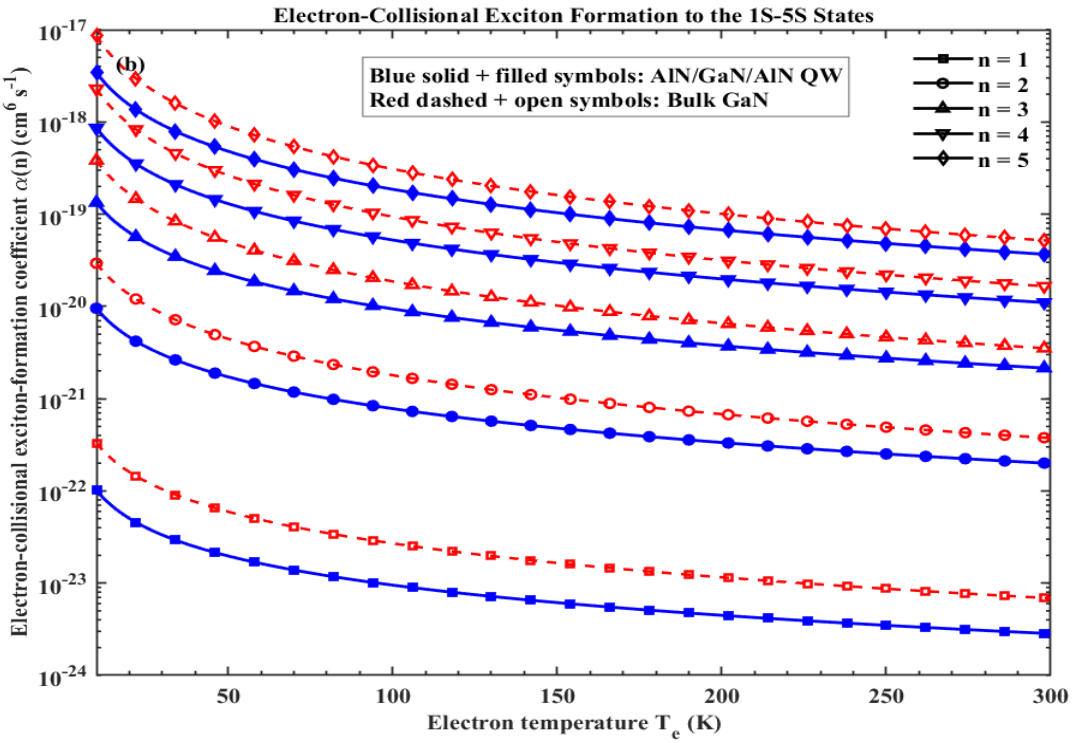


Figure.3 (b). Electron-Collisional Exciton-Formation Coefficients Versus Electron Temperature

Figure.4 illustrates the calculated 1S radiative lifetime over temperature for five electron–hole excitation-density conditions. Below about 50 K, the lifetimes remain near 0.30 ns. At higher temperatures, they increase and separate according to excitation density.

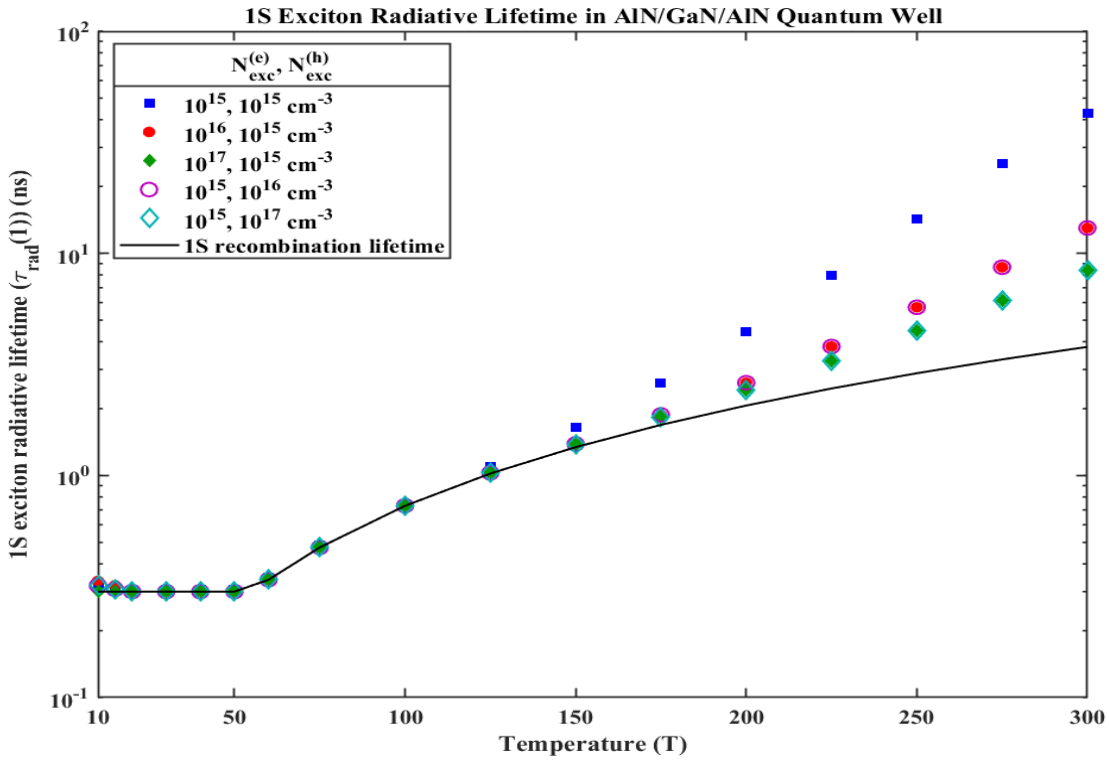
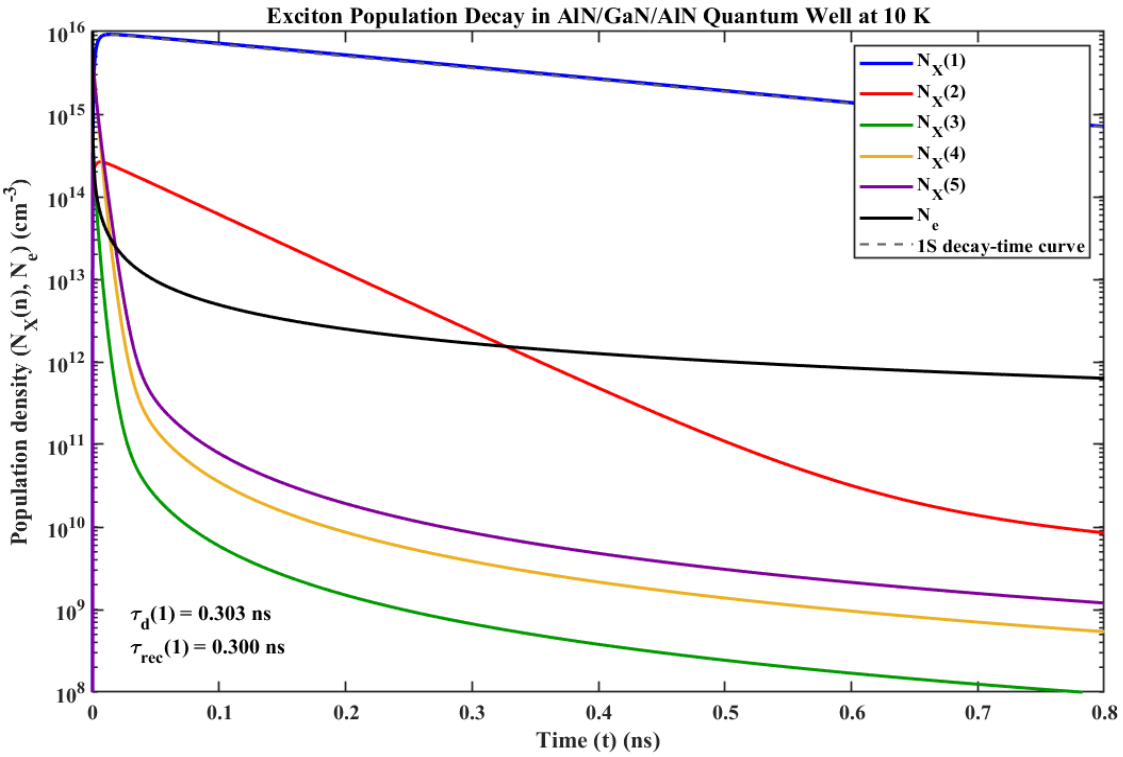
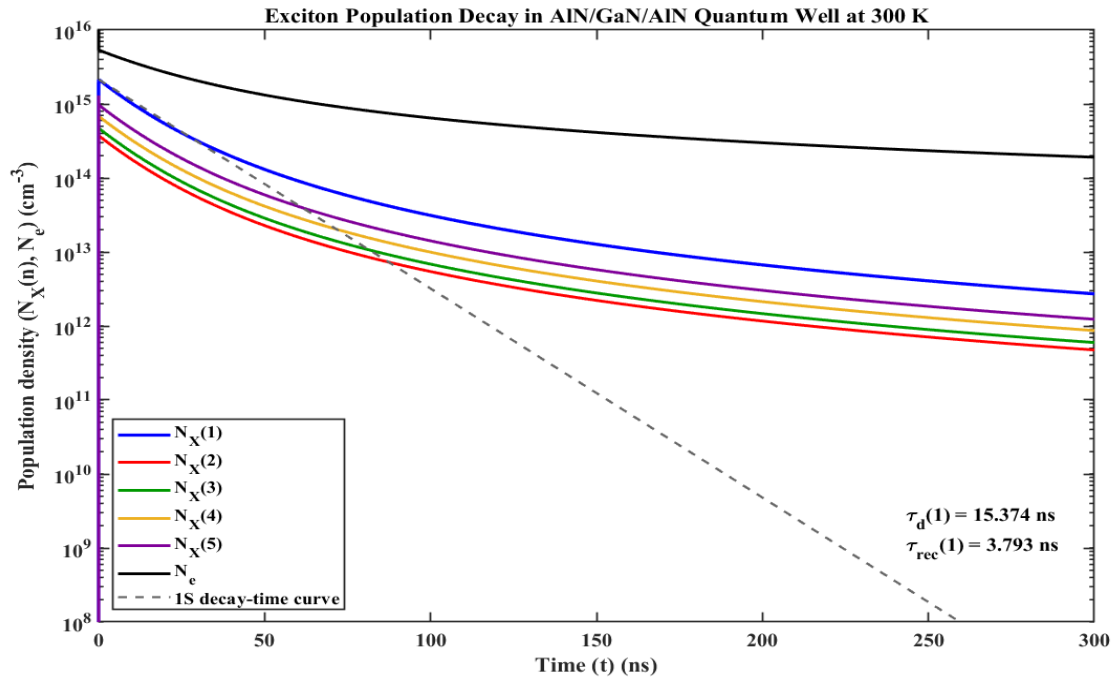


Figure.4. 1S Radiative Lifetime in the Quantum Well

Figure.5 shows the calculated 1S–5S populations and continuum after pulsed excitation. At 10 K, the 1S decay is close to the intrinsic recombination time. At 300 K, higher states and the continuum keep supplying population to 1S, making its decay slower.



(a) QW at 10 K



(b) QW at 300 K

Figure.5. Time-Dependent Exciton Populations in the Quantum Well at 10 K and 300 K

The feedback loop closes when measured structural parameters (well width, barrier thickness, interface roughness from TEM and AFM) are used to refine the model inputs, and the refined model is used to adjust the growth recipe for the next iteration. This iterative approach is standard in semiconductor process development, but the explicit linkage to phononic and excitonic physics distinguishes the present model from purely empirical optimization.

6. Energy Band Diagram of Quantum Well Semiconductor Devices

The Schrodinger equation is directly affected to the well width based on the different energy level in a single quantum well design. The detailed analysis could be done by using Finite Difference Time Domain equations. The energy band diagram of the proposed quantum well devices could be observed with different thickness of materials. The respective band structure for different layers could be found in the energy band gap. The energy band diagram of proposed quantum well solar cell is the measurement results of the energy efficiency such as internal and external performance. Factors affecting the limiting efficiency are very important to model the physical structure of quantum well semiconductor devices. Quantum well structure is suitable to design and model the high performance semiconductor devices. The structure of AlN/GaN/AlN quantum well structure is proposed in this analysis. The energy band diagram of the proposed quantum well structure based on different mole fraction has been observed the different performance. The multiquantum well design is appropriate for high performance quantum well semiconductor devices.

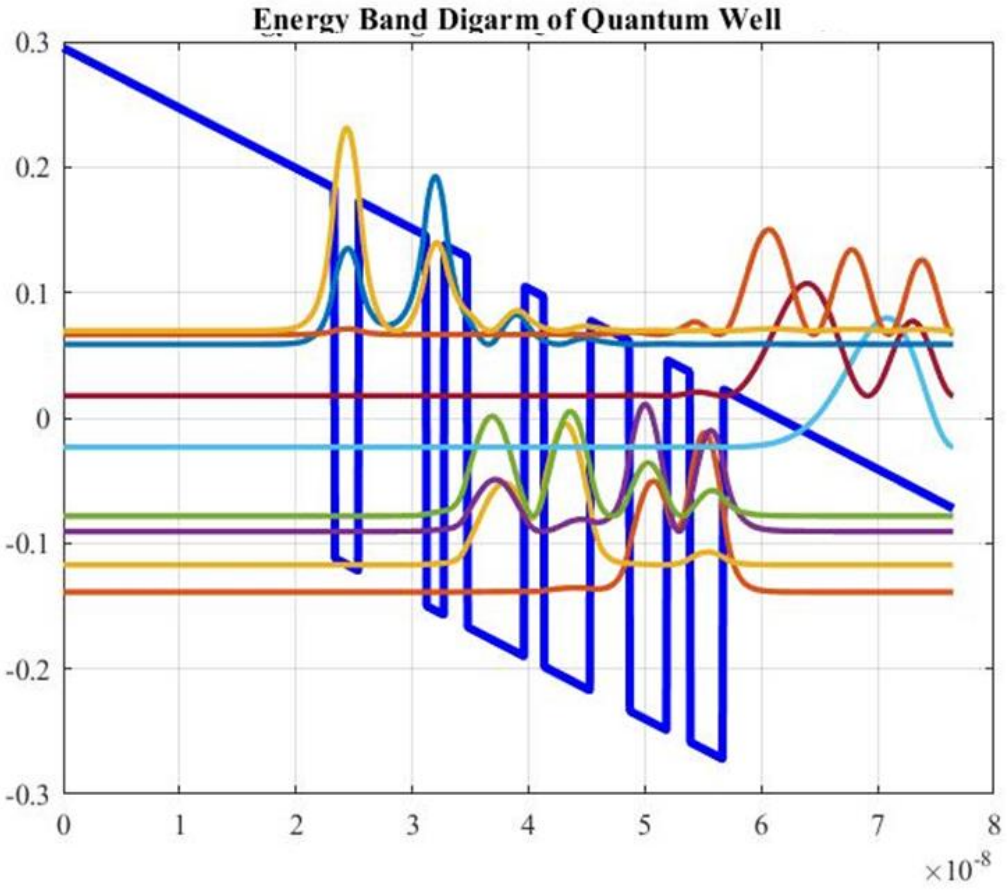


Figure.6. Energy band Diagram for Proposed QW Devcie

7. Conclusion

The AlN/GaN/AlN quantum well system provides a materials platform whose phononic, excitonic, and radiative properties are unusually well suited to THz device applications, but whose fabrication demands a level of interface control that pushes the limits of current epitaxial technology. This paper has presented a fabrication model that treats these three physical channels as coupled design variables rather than independent concerns. The key elements of the model are: (i) pre-growth modeling of phonon scattering, exciton binding, and intersubband oscillator strength to establish target layer thicknesses and tolerances; (ii) PA-MBE growth with indium-surfactant-assisted interface engineering to achieve the required abruptness; (iii) a characterization suite that validates each physical channel against measurable quantities; and (iv) an iterative feedback loop in which structural metrology refines the physical model, which in turn guides process adjustments.

REFERENCES:

[1] D. J. As, “MBE growth and applications of cubic AlN/GaN quantum wells,” Ioffe Institute, 2009.
[2] R. Paiella et al., “Intersubband device applications of nitride quantum structures,” Arizona Board of Regents, 2010.
[3] W. Lee et al., “Phonon screening of excitons in atomically thin semiconductors,” arXiv:2408.00924, 2024.
[4] J.-S. Yang et al., “Blueshift of intersubband transition wavelength in AlN/GaN multiple quantum wells by low temperature metal organic vapor phase epitaxy using pulse injection method,” Applied Physics Letters, vol. 95, no. 16, 2009.
[5] H. Zhang et al., “Indium-surfactant-assisted epitaxy of AlN/GaN/AlN resonant tunneling diodes with record peak current density,” Applied Physics Letters, vol. 118, no. 15, 2021.
[6] W. Terashima, “GaN-based terahertz quantum cascade lasers,” IEEE Xplore author profile, 2010–2020.
[7] “Intersubband transitions in nonpolar m-plane GaN/AlGaN multi-quantum-wells,” IAEA INIS Repository, 2015.
[8] L. Nevou, “Intersubband emission and modulation in nitrides nanostructures,” Ph.D. dissertation, Université Paris-Sud, 2008.
[9] “Terahertz quantum cascade lasers based on nitride semiconductors,” Chinese Academy of Sciences, Institute of Semiconductors, 2010.
[10] W. Terashima et al., “Lasing at 5.4–7 THz from GaN/AlGaN quantum cascade lasers,” IEEE Xplore, 2015.